Lawrence Berkeley National Laboratory
Recent Work

Title

PERIPHERAL THRESHOLDS AND REGGE ASYMPTOTIC EXPANSIONS

Permalink

Authors

Chew, G.F.
Koplik, J.

Publication Date

1974-05-01

LBL-3014
Preprint C.2

PERIPHERAL THRESHOLDS AND
REGGE ASYMPTOTIC EXPANSIONS

G. F. Chew and J. Koplik

May 10, 1974

DISCLAIMER

PERIPHERAL THRESHOLDS AND REGGE ASYMPTOTIC EXPANSIONS[*]

G. F. Chew and J. Koplik

Department of Physics and Lawrence Berkeley Laboratory
University of California, Berkeley, California 94720

May 10, 1974

ABSTRACT

Multiperipheral models are used to show how the Regge expansion, while lacking threshold branch points, may nevertheless approximate the localized physical effects of "peripheral" thresholds. Examples are given to demonstrate that a single pair of complex poles is capable of representing even the lowest inelastic thresholds in both total and single-particle inclusive cross sections. The Regge mechanism that allows the position of a threshold to depend sensibly on the masses of incoming and outgoing particles is elucidated.

1. INTRODUCTION

A general feature of the analytic S matrix is the occurrence in any channel invariant of a singularity at each threshold for a communicating channel. Such a singularity corresponds to the physical change that occurs when the phase space is enlarged by the opening of a new channel, but most threshold manifestations are difficult to observe and particle physicists frequently describe their data with models that ignore thresholds. Threshold effects are nevertheless always present in principle and may produce noticeable consequences even at high energy. In particular, the rising tendency of single-particle inclusive cross sections, up to ISR energies, is widely believed to be threshold-related.[1,2] It has also been suggested that the 10% increase in the pp total cross section between 20 and 60 GeV center-of-mass energy may be a threshold phenomenon.[3,4] The term "threshold" here refers not to the simple requirement that the total energy exceed the sum of the masses of produced particles, but rather to a phase-space effect associated with the peripheral character of high-energy collisions. Now at high energy Regge expansions are often employed in representation of total and inclusive cross sections, and it is natural to inquire whether such expansions are valid only to the extent that observable threshold effects have died away. The object of this paper is to discuss how the Regge expansion, even while lacking threshold branch points in a mathematical sense, may nevertheless be expected to approximate the localized physical effects of important peripheral thresholds. The material presented here is a refinement and extension of the ideas introduced in Ref. 5.

As a source of insight we shall employ multiperipheral models that are known to respect threshold kinematics, with small transverse

momentum of produced particles, while at the same time leading to Regge

asymptotic behavior. We propose to abstract from these models aspects

of the relationship between thresholds and Regge parameters that

plausibly have relevance to the physical S matrix. The role of complex

poles will be emphasized.[5]

The following questions will, in particular, be addressed:
Given the universality of Regge poles--the same set of crossed-reaction

poles describing transitions between a variety of initial and final

direct-reaction channels--what mechanism will accommodate the different

location of different direct-reaction thresholds? What Regge-pole

mechanism makes threshold effects more prominent in single-particle

inclusive cross sections than in total cross sections? When applied to

single-particle inclusive data, how do Regge parameters conform to the

common-sense expectation of increasing threshold influence with

increasing mass of the observed particle? Finally a practical but

important question: How many different complex Regge poles must be

kept in an asymptotic expansion if threshold effects are to be rep-

resented with reasonable accuracy?

2. MODEL WITH A SINGLE CROSSED CHANNEL

A. Partial and Total Cross Sections

We begin by considering the ABFST ladder model of Fig. 1, where

the "sides" of the ladder correspond to a single type of zero-spin

particle--usually identified as the pion.[6] We shall follow this latter

practice, although a literal pion identification is not important to

our objective. The "mass squared" of the "pion" is actually a

continuous (negative) momentum-transfer squared, say t_i, and each

segment of ladder sides brings a factor $S(t_i)$ which we shall refer to

as a "propagator."[7] At the same time each "rung" of the ladder

corresponds to a particle-cluster that can be produced in a "π-π

collision." Designating the square of each cluster mass by s_i, a

factor $\gamma(s_i)$ will accompany each rung; $\gamma(s_i)$ is evidently

proportional to the $\pi\pi$ cross section for producing the cluster in

question. As seen in Fig. 1, if the physical collision is between

particles A and B, the end-rungs of the ladder correspond to clusters

that can be formed in collisions between a pion and particle A or B,

respectively, and will bring factors $\gamma_A(s_A)$ and $\gamma_B(s_B)$.

It is shown in Ref. 8 that the differential cross section for

an AB collision to produce N internal clusters, as well as the two

external clusters, is then proportional to

$$F_N^{AB} = \frac{1}{\lambda^{\frac{1}{2}}(s, m_A^2, m_B^2)} \frac{(\eta - q_A - q_1 - q_2 \cdots q_N - q_B)^N}{N!} \theta(\eta - q_A - q_1 \cdots - q_B)$$

$$\times \gamma_A(s_A)S(t_1)\gamma(s_1)S(t_2)\gamma(s_2)\cdots\gamma(s_N)S(t_{N+1})\gamma(s_B) ,$$

(1)

corresponding to Fig. 1, where

$$\lambda(x,y,z) = x^2 + y^2 + z^2 - 2(xy + xz + yz),$$

(2)

$$\cosh \eta = \frac{s - m_A^2 - m_B^2}{2 m_A m_B} ,$$

(3)

$$\cosh q_i = \frac{s_i - t_i - t_{i+1}}{2(-t_i)^{\frac{1}{2}} (-t_{i+1})^{\frac{1}{2}}} ,$$

(4)

$$\sinh q_A = \frac{s_A - m_A^2 - t_1}{2m_A(-t_1)^{\frac{1}{2}}}, \tag{5}$$

$$\sinh q_B = \frac{s_B - m_B^2 - t_{N+1}}{2m_B(-t_{N+1})^{\frac{1}{2}}}. \tag{6}$$

The precise relationship between a partial cross section and F_N^{AB} is

$$\frac{d\sigma_N^{AB}}{ds_A ds_1 ds_2 \cdots ds_N ds_B dt_1 \cdots dt_{N+1}} = \frac{16\pi^3}{\lambda^{\frac{1}{2}}(s, m_A^2, m_B^2)} F_N^{AB}. \tag{7}$$

Threshold kinematics are contained in Formula (1). For example, if $N = 1$ we know that the partial cross section should vanish for

$$s < \left[(s_A)^{\frac{1}{2}} + (s_B)^{\frac{1}{2}} + (s_1)^{\frac{1}{2}} \right]^2. \tag{8}$$

This constraint is represented in Formula (1) through the θ (step) function requirement that

$$\eta > q_A + q_B + q_1, \tag{9}$$

but it is important to appreciate that Formula (8) represents an absolute threshold and is achieved only for special values of t_1, t_2 that may be quite large. The adjective "multiperipheral" reminds us that the important values of the $|t_i|$ are supposed to be small. Assuming that $|t_1|$ and $|t_2|$ are both small with respect to s_1 as well as with respect to $s_A - m_A^2$ and $s_B - m_B^2$, we have

$$q_1 \approx \log \frac{s_1}{(-t_1)^{\frac{1}{2}}(-t_2)^{\frac{1}{2}}}, \tag{4'}$$

$$q_A \approx \log \frac{s_A - m_A^2}{m_A(-t_1)^{\frac{1}{2}}}, \tag{5'}$$

and

$$q_B \approx \log \frac{s_B - m_B^2}{m_B(-t_2)^{\frac{1}{2}}}. \tag{6'}$$

It follows that

$$q_A + q_B + q_1 \approx \log \frac{s_1(s_A - m_A^2)(s_B - m_B^2)}{m_A m_B (-t_1)(-t_2)}. \tag{10}$$

In contrast to Formula (8) the threshold requirement now says that the cross section shall vanish if

$$\eta < \log \frac{(s_A - m_A^2) s_1 (s_B - m_B^2)}{(-t_1)(-t_2) m_A m_B}, \tag{11}$$

a much stronger condition.

The above is easily generalized to an arbitrary number of clusters, leading to

$$\lambda^{\frac{1}{2}}(s, m_A^2, m_B^2) F_N^{AB} \underset{\substack{\text{all } t_i \text{ small} \\ s \text{ large}}}{\approx} \gamma_A(s_A)\gamma(s_1)\cdots\gamma(s_B)S(t_1)\cdots S(t_{N+1})$$

$$\times \frac{(\eta - \Delta_N)^N}{N!} \theta(\eta - \Delta_N) \tag{12}$$

where

$$\Delta_N \approx \log \frac{(s_A - m_A{}^2)s_1 s_2 \cdots s_N (s_B - m_B{}^2)}{m_A m_B (-t_1)(-t_2)\cdots(-t_{N+1})} . \tag{13}$$

To the extent that one may speak of a mean value of $s_i t_i{}^{-1}$, the threshold for making N clusters occurs at

$$\eta_N^{thresh} \approx \log \frac{(s_A - m_A{}^2)(s_B - m_B{}^2)}{\langle -t_i \rangle \, m_A m_B} + N \log \langle \frac{s_i}{-t_i} \rangle \tag{14}$$

the interval between successive thresholds being uniform with the value

$$\Delta \approx \log \langle \frac{s_i}{-t_i} \rangle . \tag{15}$$

One-dimensional versions of the multiperipheral model incorporate thresholds uniformly spaced in η (or $\log s$) in a literal sense.[8] We shall attempt to do better in what follows, but the above qualitative analysis illustrates the threshold structure of the multiperipheral model under consideration.

Let us next look at the Regge asymptotic structure of the imaginary part of the forward AB elastic amplitude:

$$A^{AB}(\eta) = \sum_{N=0}^{\infty} \int F_N{}^{AB} ds_A \cdots ds_B dt_1 \cdots dt_{N+1} , \tag{16}$$

which is related to the total cross section by

$$\sigma_{tot}^{AB}(s) = \frac{16\pi^3}{\lambda^{\frac{1}{2}}(s, m_A{}^2, m_B{}^2)} F^{AB}(\eta) . \tag{17}$$

The individual threshold effects are now superposed. One may define the $O(1,3)$ (crossed) partial wave amplitude as

$$F^{AB}(\lambda) \equiv \int ds \, e^{-(\lambda+1)\eta(s)} F^{AB}(\eta) , \tag{18}$$

remembering that

$$\cosh \eta = \frac{s - m_A{}^2 - m_B{}^2}{2 m_A m_B} , \tag{19}$$

with the inversion rule,

$$F^{AB}(\eta) = \frac{1}{2\pi i} \int_{c-i\infty}^{c+i\infty} d\lambda \frac{e^{(\lambda+1)\eta}}{2 m_A m_B \sinh \eta} F^{AB}(\lambda) , \tag{20}$$

the contour passing to the right of all singularities of $F^{AB}(\lambda)$. If the singularities of $F^{AB}(\lambda)$ are all simple poles then we easily may obtain from Formula (20) the usual asymptotic expansion in terms of Regge-pole positions and residues.

We now are ready for an essential deduction: <u>The threshold structure of $F^{AB}(s)$ has no tendency to create singularities of $F^{AB}(\lambda)$ more complicated than simple factorizable poles.</u> Such a conclusion will allow us to argue that threshold effects in the physical S matrix are plausibly to be understood through Regge-pole parameters and do not require the introduction of less well-understood singularities.

B. Singularity Structure in the Presence of Thresholds

Singularities of the partial wave amplitude $F^{AB}(\lambda)$ are economically approached through an "amputated" amplitude $\langle t' | F(\lambda) | t \rangle$ from which $F^{AB}(\lambda)$ is obtained by a rule that corresponds to Fig. 2:

$$F^{AB}(\lambda) = \int dt \; \gamma_A(\lambda;t) S(\lambda;t) \gamma_B(\lambda;t)$$

$$+ \iint dt \; dt' \; \gamma_A(\lambda;t) S(\lambda;t) \langle t | F(\lambda) | t' \rangle S(\lambda;t') \gamma_B(\lambda;t') \; ,$$

$$\tag{21}$$

where

$$\lambda_{A,B}(\lambda;t) = \int ds_{A,B} \; e^{-(\lambda+1)q_{A,B}(s_{A,B}, m^2_{A,B}, t)} \gamma_{A,B}(s_{A,B}) \tag{22}$$

and[9]

$$S(\lambda;t) = \frac{1}{\lambda + 1} S(t) \; .$$

The amputated function satisfies the integral equation

$$\langle t' | F(\lambda) | t \rangle = \langle t' | \gamma(\lambda) | t \rangle + \int_{-\infty}^{\infty} dt'' \langle t' | \gamma(\lambda) | t'' \rangle S(\lambda;t'') \langle t'' | F(\lambda) | t \rangle \; ,$$

$$\tag{23}$$

where

$$\langle t' | \gamma(\lambda) | t \rangle = \int ds_i \; e^{-(\lambda+1)q_i(s_i, t', t)} \gamma(s_i) \; . \tag{24}$$

Illuminating theorems concerning analyticity in λ can be invoked if the integral Eq. (23) is of the Fredholm type. Conditions sufficient to ensure the latter for $\mathrm{Re}\,\lambda > -1$, are that[10]

$$\int_0^{\infty} ds_i \; \gamma(s_i) < \infty \tag{25}$$

and

$$\int_{-\infty}^{0} dt \; S(\lambda;t) < \infty \; . \tag{26}$$

Although interesting models have been proposed for which Condition (25) is not satisfied,[11] the physical effects under study in this paper are evidently related to the threshold structure of the cluster production factor, $\gamma(s_i)$, not to its asymptotic behavior for large cluster mass. Condition (26), of course, is always satisfied by any model that can be described as "multiperipheral." We should thus be on safe ground for the purposes of our investigation to apply standard Fredholm theory-- at least for $\mathrm{Re}\,\lambda > -1$.

The chief theorem to be invoked states that if both inhomogenous term and kernel of a Fredholm equation are analytic functions of a parameter, then the solution is also analytic--with the exception of poles at zeros of the Fredholm (denominator) determinant. The residues of simple poles, furthermore, are factorizable. Since Formula (24) and Condition (25) implies the analyticity of $\langle t' | \gamma(\lambda) | t'' \rangle$ in λ for $\mathrm{Re}\,\lambda > -1$, we may conclude that the only singularities of $\langle t' | F(\lambda) | t \rangle$ in the latter region are Regge poles.

Referring now to Formula (21) connecting the amputated function $\langle t' | F(\lambda) | t \rangle$ to the physical partial-wave amplitude $F^{AB}(\lambda)$ it is evident that if we assume the factors $\gamma_{A,B}(\lambda;t)$ to be analytic for $\mathrm{Re}\,\lambda > -1$, analogously to our assumption for $\langle t' | \gamma(\lambda) | t \rangle$, then $F^{AB}(\lambda)$ has only Regge pole singularities in this portion of the λ complex plane. The positions of the poles, furthermore, are the same as in the amputated function and, since the residues of the latter poles are factorizable, so will be the poles in $F^{AB}(\lambda)$. The pole residues of course depend on the incident particles, and we shall see below that this dependence is related to threshold effects.

C. A Factorizable Kernel

The integral equation (23) can be solved in closed form if the cluster factor $\langle t'|\gamma(\lambda)|t\rangle$ has a factorizable dependence on t,t'. Such a dependence does in fact obtain for t,t' small in absolute value, because then

$$e^{-q_i(s_i,t',t)} \approx \frac{(-t)^{\frac{1}{2}}(-t')^{\frac{1}{2}}}{s_i} . \tag{27}$$

Other, more accurate, factorizable approximations are available for e^{q_i}, such as

$$e^{q_i(s_i,t',t)} \approx \frac{(s_i - t)(s_i - t')}{(-s_i t)^{\frac{1}{2}}(-s_i t')^{\frac{1}{2}}} , \tag{27'}$$

but the simple form (27) will suffice for the qualitative arguments of this paper.

Let us therefore assume that the propagator $S(t)$ is negligible except for values of $|t|$ that are small compared to the cluster mass squared. Then

$$\langle t'|\gamma(\lambda)|t\rangle \approx \left[(-t')^{\frac{1}{2}}(-t)^{\frac{1}{2}}\right]^{\lambda+1} \gamma(\lambda) , \tag{28}$$

where

$$\gamma(\lambda) = \int ds_i \, s_i^{-(\lambda+1)} \gamma(s_i) , \tag{29}$$

and

$$\langle t'|F(\lambda)|t\rangle \approx \left[(-t')^{\frac{1}{2}}(-t)^{\frac{1}{2}}\right]^{\lambda+1} F(\lambda) , \tag{30}$$

with

$$F(\lambda) = \frac{\gamma(\lambda)}{1 - \gamma(\lambda)S(\lambda)} , \tag{31}$$

if

$$S(\lambda) = \int_{-\infty}^{0} dt \, S(\lambda;t)(-t)^{\lambda+1} . \tag{32}$$

The propagator-enforced restriction to small t suggests that we assume $s_A - m_A^2$ to be large compared to t so as to permit the approximation[12]

$$e^{q_A(s_A,m_A^2,t)} \approx \frac{s_A - m_A^2}{m_A(-t)^{\frac{1}{2}}} . \tag{33}$$

Then

$$\gamma_A(\lambda;t) \approx \left[m_A(-t)^{\frac{1}{2}}\right]^{\lambda+1} \gamma_A(\lambda) , \tag{34}$$

where

$$\gamma_A(\lambda) = \int ds_A \, (s_A - m_A^2)^{-(\lambda+1)} \gamma_A(s_A) , \tag{35}$$

with a corresponding approximate form for $\gamma_B(\lambda;t)$. It then follows that

$$F^{AB}(\lambda) \approx \gamma_A(\lambda)\gamma_B(\lambda)(m_A m_B)^{\lambda+1}\left[S(\lambda) + S(\lambda)F(\lambda)S(\lambda)\right]$$

$$= \frac{\gamma_A(\lambda)\gamma_B(\lambda)(m_A m_B)^{\lambda+1}S(\lambda)}{1 - \gamma(\lambda)S(\lambda)} . \tag{36}$$

To achieve maximally explicit dependence on λ, we may exhibit the singularities of $S(\lambda)$ by writing

$$S(\lambda) = \frac{1}{\lambda+1}\mathcal{J}(\lambda) , \tag{37}$$

where

$$\mathscr{S}(\lambda) \;=\; \int_{-\infty}^{0} dt \; S(t)(-t)^{\lambda+1} \;, \tag{38}$$

and finally obtain

$$F^{AB}(\lambda) \;\approx\; \frac{\gamma_A(\lambda)\,\gamma_B(\lambda)(m_A m_B)^{\lambda+1}\,\mathscr{S}(\lambda)}{\lambda + 1 - \gamma(\lambda)\mathscr{S}(\lambda)} \;. \tag{39}$$

If we choose to specify that $\gamma_{A,B}(s_{A,B})$ and $\gamma(s_i)$ decrease faster than any power for large arguments, it follows that $\gamma_{A,B}(\lambda)$ and $\gamma(\lambda)$ are analytic throughout the λ complex plane. If $S(t)$ falls faster than any power as $t \to -\infty$ [13] and approaches a constant as $t \to 0$, then the only singularities of $\mathscr{S}(\lambda)$ are simple poles at $\lambda = -2, -3, \cdots$, which cancel out in the quotient (39). Thus the only singularities of $F^{AB}(\lambda)$ are Regge poles arising from zeros of the denominator.

D. Dependence of Threshold Effects on the Incident Channel

The physical amplitude is recovered from the partial wave amplitude by the inversion rule (20), where the contour should pass to the left of a spurious pole at very large λ that is introduced by the approximation (27). A discussion of this point is given in the Appendix. If Formula (39) is expanded in powers of $\gamma(\lambda)$ to give

$$F^{AB}(\lambda) \;\approx\; \gamma_A(\lambda)\,\gamma_B(\lambda)(m_A m_B)^{\lambda+1}\,\frac{\mathscr{S}(\lambda)}{\lambda+1}\sum_{N=0}^{\infty}\left[\gamma(\lambda)\,\frac{\mathscr{S}(\lambda)}{\lambda+1}\right]^{N} , \tag{40}$$

one may identify the term of order N with the production of N internal clusters; the inversion (20) then readily yields the result (12), including the threshold step function in each partial cross section.[14]

The dependence of the total cross section on the incident channel may be neatly exhibited by substituting (39) into (20):

$$F^{AB}(\eta) \;\approx\; \iint ds_A\,ds_B\,\gamma_A(s_A)\,\gamma_B(s_B)\,\frac{1}{2\pi i}\int_c d\lambda\,\frac{e^{(\lambda+1)\eta}}{2m_A m_B\,\sinh\eta}$$

$$\times\left[\frac{m_A m_B}{(s_A - m_A^2)(s_B - m_B^2)}\right]^{\lambda+1}\frac{S(\lambda)}{1 - \gamma(\lambda)\,S(\lambda)} \tag{41}$$

or

$$2m_A m_B \sinh\eta\; F^{AB}(\eta) \;\approx\; \iint ds_A\,ds_B\,\gamma_A(s_A)\,\gamma_B(s_B)\,G\!\left(\eta - \Delta_A(s_A) - \Delta_B(s_B)\right), \tag{42}$$

where

$$G(x) \;=\; \frac{1}{2\pi i}\int_c d\lambda\,e^{(\lambda+1)x}\,\frac{S(\lambda)}{1 - \gamma(\lambda)\,S(\lambda)} \tag{43}$$

with

$$\Delta_{A,B} \;=\; \log\frac{s_{A,B} - m_{A,B}^2}{m_{A,B}} \;. \tag{44}$$

The dependence on the incident channel thus takes the form of a displacement of an otherwise universal function of η. Thresholds are correspondingly displaced, larger values of $\Delta_{A,B}$ producing higher thresholds.

How is the Regge-pole expansion affected? Writing

$$G(\eta) \;=\; \sum_i r_i\,e^{(\alpha_i+1)\eta} \;, \tag{45}$$

we have from (42)

$$F^{AB}(\eta) = \frac{e^{\eta}}{2 \sinh \eta} \sum_i g_i^A g_i^B e^{\alpha_i \eta} , \qquad (46)$$

with

$$g_i^{A,B} = \frac{(r_i)^{\frac{1}{2}}}{m_{A,B}} \int ds_{A,B} \; \gamma_{A,B}(s_B) \; e^{-(\alpha_i+1)\Delta_{A,B}(s_{A,B})} . \qquad (47)$$

A large value of $\Delta_{A,B}$ is seen to enhance the relative contribution of secondary Regge poles. High-lying thresholds, in other words, require important secondary poles.

E. Two Numerical Examples

To illustrate the foregoing, consider first a model with an internal cluster spectrum consisting of a single mass m_c. In other words,

$$\gamma(s_i) = \gamma_c m_c^2 \; \delta(s_i - m_c^2) , \qquad (48)$$

so that

$$\gamma(\lambda) = \gamma_c (m_c^2)^{-\lambda} . \qquad (49)$$

The propagator $S(t)$ will be assigned an exponential form,

$$S(t) = t_0^{-2} e^{t/t_0} , \qquad (50)$$

leading by (38) to

$$\mathscr{S}(\lambda) = (t_0)^{\lambda} \Gamma(\lambda + 2) \qquad (51)$$

and subsequently to

$$\frac{S(\lambda)}{1 - \gamma(\lambda) S(\lambda)} = \frac{t_0^{\lambda} \Gamma(\lambda + 1)}{1 - \gamma_c e^{-\lambda\Delta} \Gamma(\lambda + 1)} , \qquad (52)$$

where

$$\Delta = \log \frac{m_c^2}{t_0} . \qquad (53)$$

The Regge pole spectrum thus depends on two dimensionless parameters: γ_c and Δ. We impose a constraint on γ_c by requiring that the leading pole (the pomeron) should occur at $\lambda = 1$:

$$1 - \gamma_c \; e^{-\Delta} \Gamma(2) = 0 . \qquad (54)$$

Figure 3 then shows the real part of the positions of the next most important poles as a function of Δ, with the leading pole fixed at $\lambda = 1$. These secondary poles are complex, Fig. 4 showing the imaginary parts of their locations as a function of $1/\Delta$. Note the roughly linear relationship for large Δ, with a slope for the leading complex pair not far from the value 2π naively expected from the asymptotic oscillation hypothesis.[5,15] For extremely weak coupling (small values of γ_c) the secondary poles are real, but the condition (54) places us in a strong-coupling regime. The Appendix enlarges on this question.

The substantial spacing between the first and second pairs of complex poles encourages an attempt to represent the total cross section by an asymptotic expansion that includes no more than the leading (real) pole and the first pair of complex poles. Let us test this idea in the special case of the $\pi\pi$ total cross section, assuming m_{π}^2 to be very small compared to $s_A = s_B = m_c^2$, so that

$$\gamma_A(\lambda) = \gamma_B(\lambda) = \gamma(\lambda) . \qquad (55)$$

Further reducing the number of independent parameters by setting $t_0 = m_\pi^2$, [16] it follows from (41) that

$$F^{\pi\pi}(\eta) = \frac{1}{2\pi i} \int_c d\lambda \frac{e^{(\lambda+1)\eta}}{2 \sinh \eta} \frac{\gamma_c^2 e^{-2\lambda\Delta} \Gamma(\lambda+1)}{1 - \gamma_c e^{-\lambda\Delta} \Gamma(\lambda+1)} . \quad (56)$$

Total cross sections for incident particle combinations other than $\pi\pi$ are obtainable from (56) by the displacement rule (42).

Formula (56) may be accurately evaluated at low values of η by expanding in powers of γ_c, [17] while for a sufficiently large η the Regge asymptotic expansion becomes accurate. Our question is: What range of η is adequately represented by the pomeron plus a single pair of complex poles?

Suppose we choose $\Delta = 3$, corresponding to $m_c^2 \approx 20 t_0$. The first pair of complex poles then is situated at $\alpha_c = 0.30 \pm 2.6 i$, and the associated Regge approximation to $\sigma_{\pi\pi}^{tot}$ is shown in Fig. 5 plotted as a function of $\log s \approx \eta + \log m_\pi^2$, with the exact behavior shown for comparison. One observes that the asymptotic expansion gives an accurate picture down to the threshold for the first internal cluster and is qualitatively meaningful all the way down to the lowest threshold. In Ref. 5 a multiperipheral threshold example analogous to the foregoing was studied but with the unrealistically abrupt thresholds characteristic of strictly one-dimensional models. Here we have smoothed out the thresholds by attending to the coupling between transverse and longitudinal degrees of freedom and once again have found powerful capacity in a single pair of complex poles.

It is plausible from the asymptotic oscillation concept that a single pair of complex poles might do a good job of approximating a

model characterized by a single period Δ. But the actual cluster spectrum must contain a range of masses and thus a range of Δ. Let us look next therefore at a model with two different internal cluster-masses m_c and $m_{c'}$, although the external clusters are still restricted to m_c. We continue to assume the propagator $S(t)$ to be universal. With an obvious notation we find in place of (56)

$$F^{\pi\pi}(\eta) = \frac{1}{2\pi i} \int_c d\lambda \frac{e^{(\lambda+1)\eta}}{2 \sinh \eta} \frac{\gamma_c^2 e^{-2\lambda\Delta} \Gamma(\lambda+1)}{1 - (\gamma_c e^{-\lambda\Delta} + \gamma_{c'} e^{-\lambda\Delta'}) \Gamma(\lambda+1)} .$$

$$(57)$$

Let us choose $\Delta = 2$ and $\Delta' = 4$, and continue to insist on a pomeron at $\lambda = 1$. Let us furthermore put the major burden for the multiperipheral mechanism on the lower mass by choosing

$$\frac{\gamma_{c'} e^{-\Delta'}}{\gamma_c e^{-\Delta}} = 0.25.$$

In this case, not surprisingly, the Regge pole spectrum becomes more complicated: the leading pair of complex poles occurs at $0.05 \pm 1.6 i$ while the next is somewhat closer than previously, at $-0.43 \pm 3.4 i$. In Fig. 6 we compare the exact cross section to the asymptotic expansion with either one or two complex pole pairs retained. We see that in both cases the agreement is as good as in the one-cluster case, and further that inclusion of the second pair is not really necessary for $\log s \gtrsim -1$. The imaginary part of the leading pole residue corresponds to an oscillation period of 4.0 units in η, so only the threshold effect of the heavier mass is significant once moderate energies are reached.

F. Single-Particle Inclusive Cross Section

The single-particle inclusive cross section for $A + B \rightarrow C + X$ depends on three variables which for our purpose are conveniently chosen, in the way advocated by Mueller,[18] to be ζ_A, ζ_B and θ, where

$$\cosh \zeta_A = \frac{p_A \cdot p_C}{m_A m_C}$$

and

$$\cosh \zeta_B = \frac{p_B \cdot p_C}{m_B m_C} , \tag{58}$$

while θ is the angle between $\vec{p}_A$ and $\vec{p}_B$ in the rest frame of C. In the foregoing discussion of the total cross section we have used a variable η such that

$$\cosh \eta = \frac{p_A \cdot p_B}{m_A m_B} ,$$

and it is easy to show that

$$\cosh \eta = \cosh \zeta_A \cosh \zeta_B + \sinh \zeta_A \sinh \zeta_B \cos \theta . \tag{59}$$

Evidently, when θ vanishes so does the transverse momentum of the observed particle in a frame where p_A and p_B are colinear.[19] Thus small values of the conventionally-defined transverse momentum mean small values of θ and the approximate connection $\eta \approx \zeta_A + \zeta_B$.

The single-particle inclusive cross section is related to an invariant amplitude $\mathscr{F}_C^{AB}(\zeta_A, \zeta_B, \theta)$ by the same flux factor that relates $F^{AB}(\eta)$ to the total cross section, and by analogy to (20) one may expand $\mathscr{F}_C^{AB}$ in terms of matrix elements of the irreducible representations of the Lorentz group. The advantage of Mueller's variables is their natural role in this expansion. As shown by

Bassetto, Toller and Sertorio,[20] the result is

$$\mathscr{F}_C^{AB}(\zeta_A, \zeta_B, \theta) = \int_C d\lambda \int_C d\lambda' \sum_j d_{00j}^{0,\lambda+1}(\zeta_A) P_j(\cos \theta) d_{0j0}^{0,\lambda+1}(\zeta_B)$$
$$\times \mathscr{F}_C^{AB}(\lambda, \lambda'; j) . \tag{60}$$

To reduce the discussion from 3 variables to 2, we project out the $j = 0$ component, defining

$$\mathscr{F}_C^{AB}(\zeta_A, \zeta_B) = \frac{1}{2} \int_{-1}^{+1} d\cos\theta \, \mathscr{F}_C^{AB}(\zeta_A, \zeta_B, \theta) , \tag{61}$$

an operation roughly equivalent to integration over the transverse momentum of particle C. Small average transverse momentum means that most of the contribution to (61) will come from the neighborhood of $\cos \theta = 1$, so we may make the rough identification

$$\eta \approx \zeta_A + \zeta_B . \tag{62}$$

In any event, if (60) is substituted into (61) and explicit forms are inserted for the group representation functions, we find

$$\mathscr{F}_C^{AB}(\zeta_A, \zeta_B) = \text{constant} \times \int_C d\lambda \int_C d\lambda'$$
$$\times \frac{e^{(\lambda+1)\zeta_A}}{(\lambda+1)\sinh \zeta_A} \frac{e^{(\lambda'+1)\zeta_B}}{(\lambda'+1)\sinh \zeta_B} \mathscr{F}_C^{AB}(\lambda,\lambda';0). \tag{63}$$

The preceding formulae are general, physical results being obtained if something is known about the singularities of $\mathcal{G}_C^{AB}(\lambda, \lambda'; 0)$. Mueller made the hypothesis that the poles of inclusive amplitudes are universal and thus the same as those that control total cross sections.[18] Multiperipheral models go further and give explicit relations between $\mathcal{F}_C^{AB}(\lambda, \lambda'; 0)$ and $F^{AB}(\lambda)$. For the above-described single-channel model, if we define "one-sided" functions

$$F^A(\lambda;\ t)\ =\ \gamma_A(\lambda;\ t)\ +\ \int dt'\ \gamma_A(\lambda;\ t')\ S(\lambda;\ t')\langle t'\ |F(\lambda)|\ t\rangle \tag{64}$$

and

$$F^B(\lambda;\ t)\ =\ \gamma_B(\lambda;\ t)\ +\ \int dt'\ \langle t|F(\lambda)|t'\rangle\ S(\lambda;\ t')\ \gamma_B(\lambda;\ t')\ , \tag{65}$$

such that

$$
\begin{aligned}
F^{AB}(\lambda)\ &=\ \int dt\ F^A(\lambda;\ t)\ S(\lambda;\ t)\ \gamma_B(\lambda;\ t) \\
&=\ \int dt\ \gamma_A(\lambda;\ t)\ S(\lambda;\ t)\ F^B(\lambda;\ t)\ ,
\end{aligned} \tag{66}
$$

Bassetto, Sertorio and Toller[20] have shown that

$$
\begin{aligned}
\mathcal{F}_C^{AB}(\lambda,\ \lambda';\ 0)\ =\ \text{constant} \times \int\!\!\int dt'\ dt\ \ \frac{F^A(\lambda;\ t)}{m_A(-t)^{\frac{1}{2}}}\ S(t) \\
\times\ \frac{e^{-(\lambda+1)\beta}}{\cosh \beta}\ \lambda^{\frac{1}{2}}(m_C^2, t, t')\ \frac{e^{-(\lambda'+1)\beta'}}{\cosh \beta'}\ S(t')\ \frac{F^B(\lambda';\ t')}{m_B(-t')^{\frac{1}{2}}}
\end{aligned} \tag{67}
$$

where

$$\sinh \beta\ =\ \frac{m_C^2 + t - t'}{2m_C(-t)^{\frac{1}{2}}}\ , \tag{68}$$

$$\sinh \beta'\ =\ \frac{m_C^2 + t' - t}{2m_C(-t')^{\frac{1}{2}}}\ . \tag{69}$$

This formula is illustrated in Fig. 7. In our multiperipheral model, therefore, the only λ singularities of the single-particle inclusive amplitude are those Regge poles that already appear in the total cross section. Just as for the latter quantity, threshold effects must be representable through secondary Regge poles.

Use of the small-t factorization approximation further illuminates the physical situation. Suppose we replace (68) by

$$e^\beta\ \approx\ \frac{m_C}{(-t)^{\frac{1}{2}}}\ , \tag{70}$$

so

$$\frac{e^{-(\lambda+1)\beta}}{\cosh \beta}\ \approx\ 2\left(\frac{m_C}{(-t)^{\frac{1}{2}}}\right)^{-(\lambda+2)}\ . \tag{71}$$

A corresponding approximation for β', together with

$$\lambda^{\frac{1}{2}}(m_C^2,\ t,\ t')\ \approx\ m_C^2$$

and

$$F^{A,B}(\lambda,\ t)\ \approx\ \left(m_{A,B}(-t)^{\frac{1}{2}}\right)^{\lambda+1}\ F^{A,B}(\lambda)\ , \tag{72}$$

leads to

$$\mathcal{F}_C^{AB}(\lambda,\ \lambda';\ 0)\ \approx\ \mathcal{F}_C^A(\lambda)\ \mathcal{F}_C^B(\lambda')\ , \tag{73}$$

where

$$\mathcal{F}_C^{A,B}(\lambda) \approx \text{constant} \times \left(\frac{m_{A,B}}{m_C}\right)^\lambda F^{A,B}(\lambda)\,\mathcal{I}(\lambda)\,. \tag{74}$$

Correspondingly,

$$\mathcal{F}_C^{AB}(\zeta_A, \zeta_B) \approx \mathcal{F}_C^A(\zeta_A)\,\mathcal{F}_C^A(\zeta_B)\,, \tag{75}$$

where

$$\mathcal{F}_C^{A,B}(\zeta_{A,B}) \approx \text{constant} \times \int_c d\lambda\; \frac{e^{(\lambda+1)\zeta_{A,B}}}{\sinh \zeta_{A,B}}\; \left(\frac{m_{A,B}}{m_C}\right)^\lambda S(\lambda) F^{A,B}(\lambda)\,. \tag{76}$$

Now, since

$$F^{A,B}(\lambda) = \int s_{A,B}\; \gamma_{A,B}(s_{A,B})\; \frac{\left(s_{A,B} - m_{A,B}^2\right)^{-(\lambda+1)}}{1 - \gamma(\lambda) S(\lambda)}\,,$$

the dependence on the incident channel will follow the same displacement rule as for the total cross section. There is a similar rule for the dependence on the mass of the observed produced particle, any threshold structure being displaced in ζ_A or ζ_B by an interval $\log m_{C'}/m_C$ if the observed mass is changed from m_C to $m_{C'}$.[21]

Having understood the dependence on the masses of incident and produced particles, it will suffice to consider incident pions and a produced particle whose mass m_C is the same as that of an external cluster. Straightforward calculation leads to

$$\sinh \zeta_A\, \mathcal{F}_C^\pi(\zeta_A) \propto \sinh\!\left(\zeta_A + \log \frac{m_C}{m_\pi}\right) F^{\pi\pi}\!\left(\zeta_A + \log \frac{m_C}{m_\pi}\right)\,.$$

In our model with a single crossed channel, in other words, the threshold structure in the separate variables ζ_A and ζ_B follows that in the total cross section (with an appropriate displacement).

It must be remembered, of course, that the single-particle inclusive cross section is given by a product of two factors, one depending on ζ_A and the other on ζ_B, with the approximate relation $\zeta_A + \zeta_B \approx \eta$, so the net energy dependence of the single-particle inclusive cross section will exhibit a different threshold structure from that in the total cross section, although the two structures are related to each other.

In particular, our demonstration that a single pair of complex poles can give a good representation of threshold effects in the total cross section can be immediately extended to single-particle inclusive cross sections. Figure 8 shows the latter, evaluated at the symmetric point $\zeta_A = \zeta_B = \eta/2$ for the single cluster-mass example described in Sec. II.D. The curve shows an asymptotic expansion for $\pi\pi$ collisions involving pomeron-pomeron plus pomeron-complex pole terms; a further refinement would include the complex pole-complex pole term, but this turns out to be a small correction. Note that the first peak in the inclusive cross section occurs at the same energy as that from the one-cluster contribution to the total cross section in Fig. 5.

It is also instructive to calculate the inclusive cross section for the two-cluster case described in Sec. II.D, and in Fig. 9 we show the results for both light and heavy clusters. As expected, the threshold for the heavy cluster spectrum is delayed by approximately two units of $\log s$, while the asymptotic height of the large-cluster

inclusive cross section is roughly 1/4 that of the light cluster. The shorter-wavelength oscillation with a period of 2 units that one would naively have expected in the light-cluster cross section is almost invisible, only the long-wavelength heavy-cluster-induced oscillation being apparent. Note also that the amplitude of the oscillation in the two-cluster example is smaller than for the single-cluster model.

3. CONCLUSION

A simplifying feature of the foregoing multiperipheral examples has been the single crossed channel with a factorizable kernel. Are qualitatively different results to be expected from a more realistic kernel? Guaranteed to survive any kernel complication is the capacity of secondary Regge poles to represent threshold effects, so long as the multiperipheral equation maintains a Fredholm character. One cannot prove that the important secondary poles are complex, and in Ref. 22 a two-channel model is described where the important secondary poles are real if the interchannel coupling is weak. These poles become complex for strong coupling, however, and threshold effects turn out to be insignificant in the weak coupling regime. We are unaware of counter-examples to the proposition that Regge expansions accommodate physically significant peripheral thresholds through complex poles.

Nonfactorizable kernels tend to produce a higher density of poles,[23] and there can be no general assurance that retention of only a few poles will adequately represent the threshold region. The simple models of this paper nevertheless encourage attempts to fit threshold

data with the leading real pole(s) plus a single complex pair. In our examples not only total cross sections but also single-particle inclusive cross sections are well represented by such an approximation, and there is every reason to suppose the same to be true for other physical observables such as mean particle multiplicity.[24]

We shall finally comment on the relation of the models discussed here to ABFST models where the propagator is strictly that of Footnote 7. Although the unmodified propagator has been shown to give complex poles,[25,26] they are so far to the left in the λ plane as to be physically uninteresting.[27] Some modification of the propagator to reduce large-$|t|$ contributions is essential to the generation of substantial peripheral-threshold effects.

ACKNOWLEDGMENT

FOOTNOTES AND REFERENCES

* This work was supported in part by the U. S. Atomic Energy
Commission.

1. L. Caneschi, Nucl. Phys. $\underline{B68}$ (1974) 77.

2. R. Blutner, Karl Marx University preprint KMU-HEP-7311 (1973).

3. M. Suzuki, Nucl. Phys. $\underline{B69}$ (1974) 486.

4. T. Gaisser and C. I Tan, Phys. Rev. $\underline{D8}$ (1973) 3881.

5. G. F. Chew and D. R. Snider, Phys. Letters $\underline{31B}$ (1970) 75.

6. L. Bertocchi, S. Fubini and M. Tonin, Nuovo Cim. $\underline{25}$ (1962) 626 ;
   D. Amati, S. Fubini and A. Stanghellini, ibid., $\underline{26}$ (1962) 896.

7. With no off-shell modification the pion propagator would be

$$S(t) = 1/(t - m_\pi^2)^2 ,$$

but we shall assume a faster rate of decrease as $|t|$ becomes
large.

8. G. F. Chew, T. Rogers and D. R. Snider, Phys. Rev. $\underline{D2}$ (1970) 765.

9. The factorization of the λ and t dependence in $S(\lambda; t)$
   results from our assumption that the ladder sides are built from
   particles of zero spin. In a more general model with Reggeon
   sides, the rightmost λ singularity of the propagator would
   occur at $\lambda = 2\alpha_R(t) - 1$.

10. To obtain these conditions, first note that the preceding devel-
    opment can easily be modified so as to employ the symmetric
    kernel

$$K(t',t'') = \left[S(\lambda;t') \, S(\lambda;t'') \right]^{\frac{1}{2}} \langle t' | \gamma(\lambda) | t'' \rangle .$$

Then in (24), since q_i is positive we have for $\text{Re } \lambda > -1$ that
$|\exp[-(\lambda+1)q_i]| < 1$, so

$$|\langle t'|\gamma(\lambda)|t''\rangle| < \int_0^\infty ds_i \, \gamma(s_i) .$$

The basic condition for the Fredholm theorem is square integrability,

$$\iint_{-\infty}^{0} dt' \, dt'' \, |K(t', t'')|^2 < \infty ,$$

which is ensured by (25-26).

11. For example, models that include the high subenergy pomeron "tail"
    of the elastic $\pi\pi$ cross section.

12. This assumption is in no way essential to our arguments, but makes
    various formulas more transparent.

13. This restriction is made only to simplify the argument. We have
    verified by numerical integration of the exact equations (1) - (7)
    that a propagator which decreases as a sufficiently large power of
    t suffices to generate important threshold effects in the total
    cross section.

14. Straightforward calculation reveals that if $\eta < \triangle_N$ the function
    $F_N^{AB}(\lambda)$ decreases exponentially as $\text{Re } \lambda \to +\infty$. The contour
    integral in (20) may then be completed to the right, encircling
    no singularities and thus yielding the result zero.

15. G. F. Chew and J. Koplik, Phys. Letters $\underline{48B}$ (1974) 221.

16. From Eq. (50) we see that this value corresponds to perhaps
    unreasonably strong damping in momentum transfer. The necessity
    of this choice can be traced back to the fact that both the
    approximation (27) for e^{-q_i} and the resulting kernel function

(28) increase with t. This property is not shared by the exact

form of e^{-q_i} or by the alternate approximation given in (27'),

and had we used either of these a more sensibly damped propagator

would have given physically equivalent results.

17. Because of the failure at large $|t|$ of approximations such as

(27), absolute thresholds such as (8) have been lost from (56).

Our exponential suppression of large $|t|$ nevertheless guarantees

that at a finite value of η only a finite number of terms can

be appreciable in the γ_c power expansion.

18. A. H. Mueller, Phys. Rev. D2 (1970) 2963.

19. If ζ_A and ζ_B are both large, one may show that

$$\tan \Theta/2 \approx p_{C\perp}/m_C ,$$

where $p_{C\perp}$ is the transverse momentum of particle C in the

center-of-mass frame of particle A and B.

20. A. Bassetto, M. Toller and L. Sertorio, Nucl. Phys. B35 (1971) 1.

21. Papers by Caneschi[1] and by Blutner[2] have emphasized the

multiperipheral-model prediction of a threshold-region increase

in the single-particle inclusive cross section, the effective

threshold increasing with the mass of the produced particle. The

approximations employed in these papers, however, attribute the

threshold structure to kinematic "daughter" poles of the pomeron,

not shared by other amplitudes. As our arguments above indicate,

a consistent analysis within the multiperipheral model requires

that the energy dependence of inclusive spectra, and threshold

effects in particular, be expressed in terms of the same Regge

poles appearing in the total cross section.

22. J. Koplik, LBL-3022 (1974).

23. Symmetries such as isospin may permit partial diagonalization of
the kernel. All statements in this paper should be understood
as referring to a well-defined set of good quantum numbers for
the crossed channel.

24. M. L. Goldberger, D. Silverman and C.-I Tan, Phys. Rev. Letters
26 (1971) 100.

25. M. N. Misheloff, Phys. Rev. D3 (1971) 1486.

26. S.-S. Shei, Phys. Rev. D3 (1971) 1962.

27. H. W. Wyld, Jr., Phys. Rev. D3 (1971) 3090.

28. Y. I. Azimov, A. A. Ansel'm, and V. M. Shekhter, Zh. Eksp. Teor.
Fiz. 44 (1963) 361, 1078 [Soviet Physics-JETP 17 (1963) 246, 726];
N. F. Bali, S.-Y. Chu, R. W. Haymaker, and C.-I Tan, Phys. Rev.
161 (1967) 1450.

29. M. Bishari, private communication (1973).

30. E. Hille, Analytic Function Theory, Vol. I (Ginn and Co., 1959).

APPENDIX

The Weak-Coupling Limit and Spurious Poles

While the models we have discussed are physically relevant only in the case of "strong coupling," when the strength of the kernel is sufficient to generate a Regge pole near $\lambda = 1$, it is none the less instructive to study the motion of the poles as the coupling varies. In particular, we will show that in the weak-coupling limit all poles retreat to negative integer values of λ, and that complex poles only result from the collision of real poles, just as in potential scattering.[28]

For definiteness, we will study the single-cluster model with exponential damping in $|t|$, described in Sec. 2.E. Using Eqs. (36), (37), (49) and (51), we can write $F^{AB}(\lambda)$ as an exponential in λ divided by

$$D(\lambda) \equiv \Gamma^{-1}(\lambda + 1) - \gamma_c e^{-\Delta\lambda} . \qquad (A.1)$$

Regge poles occur at values of λ for which this expression vanishes. If $\gamma_c = 0$, these zeros occur at $\lambda = -1, -2, \cdots$. In Fig. 10 we plot separately the two terms in $D(\lambda)$ for real values of λ. If γ_c is small (lower dashed curve) the zeros shift slightly in position-- the leading one at $\lambda = -1$ moves to the right, the next two at $\lambda = -2$ and -3 move towards each other, and so on, with all lower-lying zeros approaching each other in pairs. As γ_c increases this trend continues until at a sufficiently large coupling some of the pairs may collide and move off into the complex λ-plane (upper dashed curve). When γ_c is large enough for the leading zero to have reached $\lambda = 1$ (when (54) is satisfied) the leading secondary zeros have moved to the

positions shown in Figs. 3 and 4. Zeros which began sufficiently far to the left continue to be real however; this result follows from the fact that the amplitude of the oscillation in $\Gamma^{-1}(\lambda + 1)$ increases faster than any exponential as λ decreases (a property easily derived from Stirling's formula) and for sufficiently negative λ the two terms in $D(\lambda)$ continue to intersect at real points.

To conclude that the only zeros are those which began at negative integer points for $\gamma_c = 0$, it remains only to show that none could have moved in from infinity. The argument which follows[29,30] is based on Rouché's theorem of complex analysis. Suppose we have a simple, closed, connected curve L and two functions $f(z)$ and $g(z)$ which are meromorphic within L, and on L are analytic, nonvanishing, and satisfy

$$|g(z)/f(z)| < 1 .$$

The theorem states that the difference between the number of zeros and the number of poles inside L is the same for both functions $f(z)$ and $f(z) + g(z)$. In our application we identify f and g with $\Gamma^{-1}(\lambda + 1)$ and $-\gamma_c e^{-\Delta\lambda}$, respectively, and choose L to be the curve shown in Fig. 11: a semi-circle to the left of $\lambda = -1$ extended to the right as far as C, the contour along which the inverse Laplace transform (20) is taken. Along the semi-circular arc, excluding a narrow interval about the negative real axis, Stirling's formula implies directly that for sufficiently large radius

$$|-\gamma_c e^{-\Delta\lambda} \Gamma(\lambda + 1)| < 1 . \qquad (A.2)$$

Near the real axis (A.2) is not correct in general due to the poles of Γ; we first write

$$\Gamma(\lambda + 1) = \pi \left[\sin \pi(-\lambda) \, \Gamma(-\lambda) \right]^{-1}$$

and choose L to cross the axis at a negative half-integer value of λ. Then $|\sin \pi(-\lambda)| \simeq 1$ near the real axis, and using the asymptotic expansion of $\Gamma(-\lambda)$ we obtain (A.2). Along the horizontal segments of L we again use Stirling's formula, and find that (A.2) is satisfied provided L does not extend too far to the right. This is really no restriction at all, since we shall show below that the inversion contour C must be located in a region of the λ-plane for which (A.2) holds. Therefore (A.2) is satisfied on all of L, and Rouché's theorem implies that $D(\lambda)$ has the same number of zeros within L as $\Gamma^{-1}(\lambda + 1)$. Since L can be taken arbitrarily far to the left, the interior of L can be extended to the entire region to the left of the inversion contour C, and thus no additional zeros can appear from infinity.

A subtlety involved in the construction of the asymptotic expansion in this model requires some discussion. Recall that the process by which we have obtained the amplitude as a function of λ may be represented schematically as

$$F(\lambda) \equiv \int ds \, e^{-(\lambda+1)\eta(s)} \sum_N F_N(s)$$

$$= \sum_N \int ds \, e^{-(\lambda+1)\eta(s)} F_N(s)$$

$$= \sum_N F_N(\lambda) , \qquad (A.3)$$

where $F_N(s)$ is proportional to the cross section for N particle-clusters. For this expression to be mathematically sensible we require (at the least) that the final summation converge. This sum is just a geometric series in which the ratio of successive terms is the kernel

$$K(\lambda) \equiv \frac{1}{\lambda + 1} \, \gamma(\lambda) \, \mathscr{S}(\lambda) ,$$

so we require that the modulus of this quantity be less than one. In the particular model discussed in this Appendix and in Sec. 2.E we have

$$K(\lambda) = \gamma_c \, e^{-\Delta\lambda} \, \Gamma(\lambda + 1) ,$$

and thus we must consider the amplitude for values of λ for which $|K(\lambda)| < 1$; i.e., (A.2) is satisfied.

This is an important restriction here because in addition to what we have referred to as the "leading" real pole, it is easy to show that there always exists another real pole further to the right, with a negative residue. The latter pole does not contribute to the asymptotic expansion, however: the correct procedure is to carry out (A.3) for a value of λ for which (A.2) holds, which requires $\mathrm{Re}(\lambda)$ to be between the above two real poles, and then to invert the transform according to (20). When the contour is then closed to the left to obtain the asymptotic expansion (the integrand in (20) diverges if $\mathrm{Re}(\lambda) \rightarrow + \infty$), the second real pole does not contribute. This difficulty is usually not present in multiperipheral models; it occurs here because the kernel $K(\lambda)$ increases as $\mathrm{Re}(\lambda) \rightarrow +\infty$, a peculiarity of the bad large-$|t|$ behavior of the approximation (27).[16]

FIGURE CAPTIONS

Fig. 1. Multiperipheral diagram defining the variables in Formula (1).

Fig. 2. Schematic representation of Eq. (21).

Fig. 3. The real parts of the positions of the leading complex poles of Formula (52) subject to the constraint (54).

Fig. 4. The imaginary parts of the positions of the poles appearing in Fig. 3.

Fig. 5. The total and partial cross sections corresponding to Formula (56), subject to the constraint (54), with $\eta = \log s/m_\pi^2$ and $\Delta = 3$. The asymptotic expansion includes the leading real pole at $\lambda = 1$ and the first pair of complex poles at $\lambda = 0.30 \pm 2.6\, i$.

Fig. 6. The total cross section corresponding to Formula (57), with $\Delta = 2$, $\Delta' = 4$ and γ_c, $e^{-\Delta'} = 0.25\, \gamma_c\, e^{-\Delta}$. The parameter γ_c is chosen to place the leading real pole at $\lambda = 1$. The asymptotic approximations correspond to one pair or two pairs of complex poles, located at $\lambda = 0.05 \pm 1.6\, i$ and $\lambda = -0.43 \pm 3.4\, i$.

Fig. 7. Schematic representation of Formula (67).

Fig. 8. The central-region single-cluster inclusive cross section corresponding to the total cross section shown in Fig. 5.

Fig. 9. The central-region single-cluster inclusive cross sections corresponding to the total cross section shown in Fig. 6.

Fig. 10. The separate terms in $D(\lambda)$ as a function of (real) λ.

Fig. 11. Contour for application of Rouché's theorem.
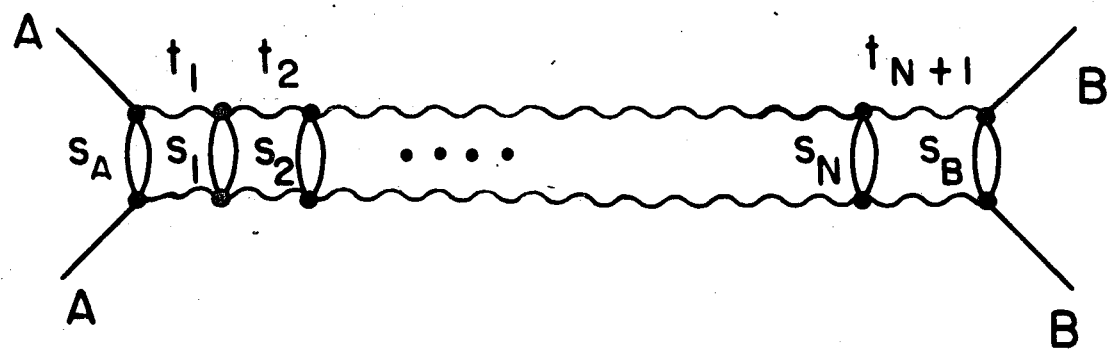
Fig. 1.

XBL745-3052

Fig. 2.

XBL745-3053

Fig. 3

XBL745-3054

-39-
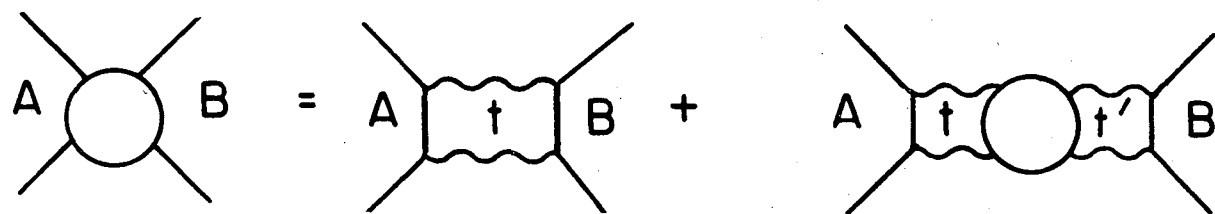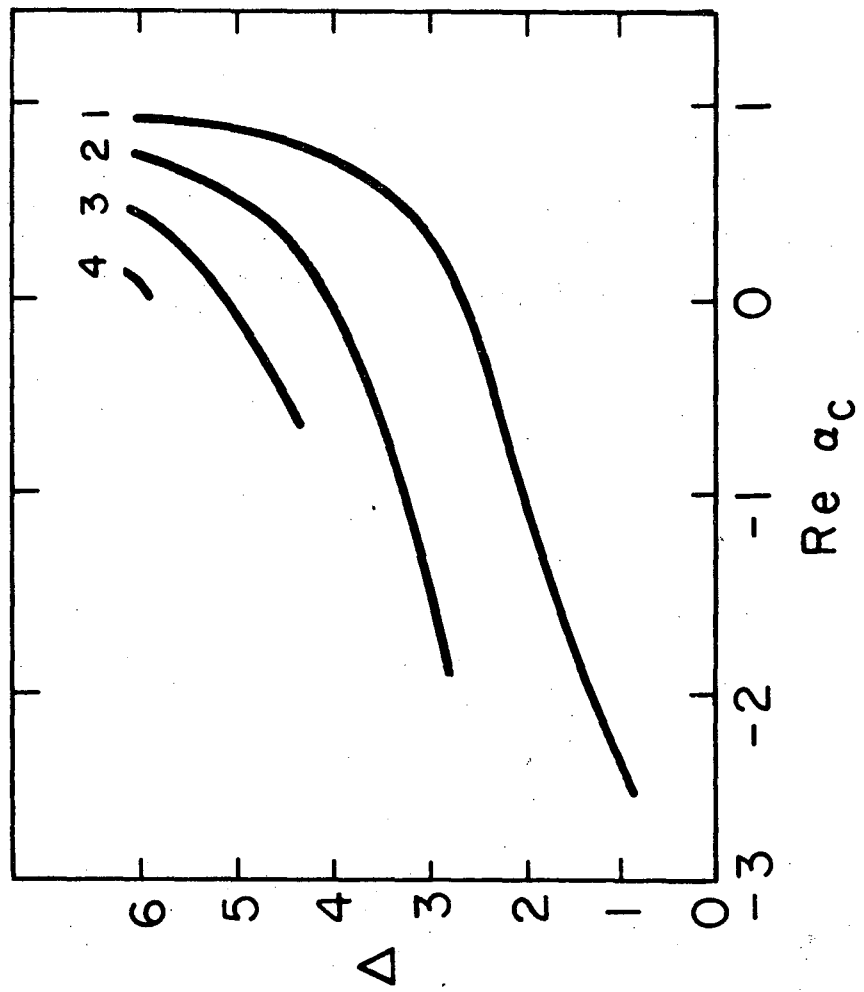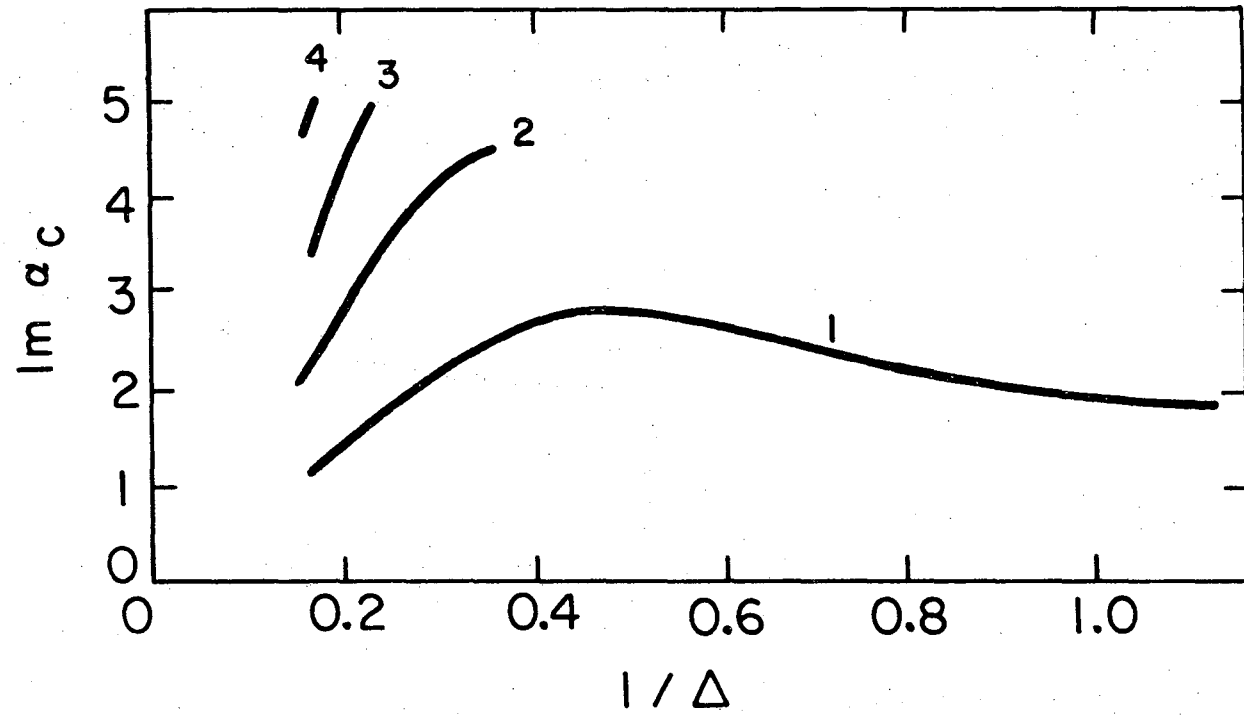
XBL745-3055

Fig. 4.
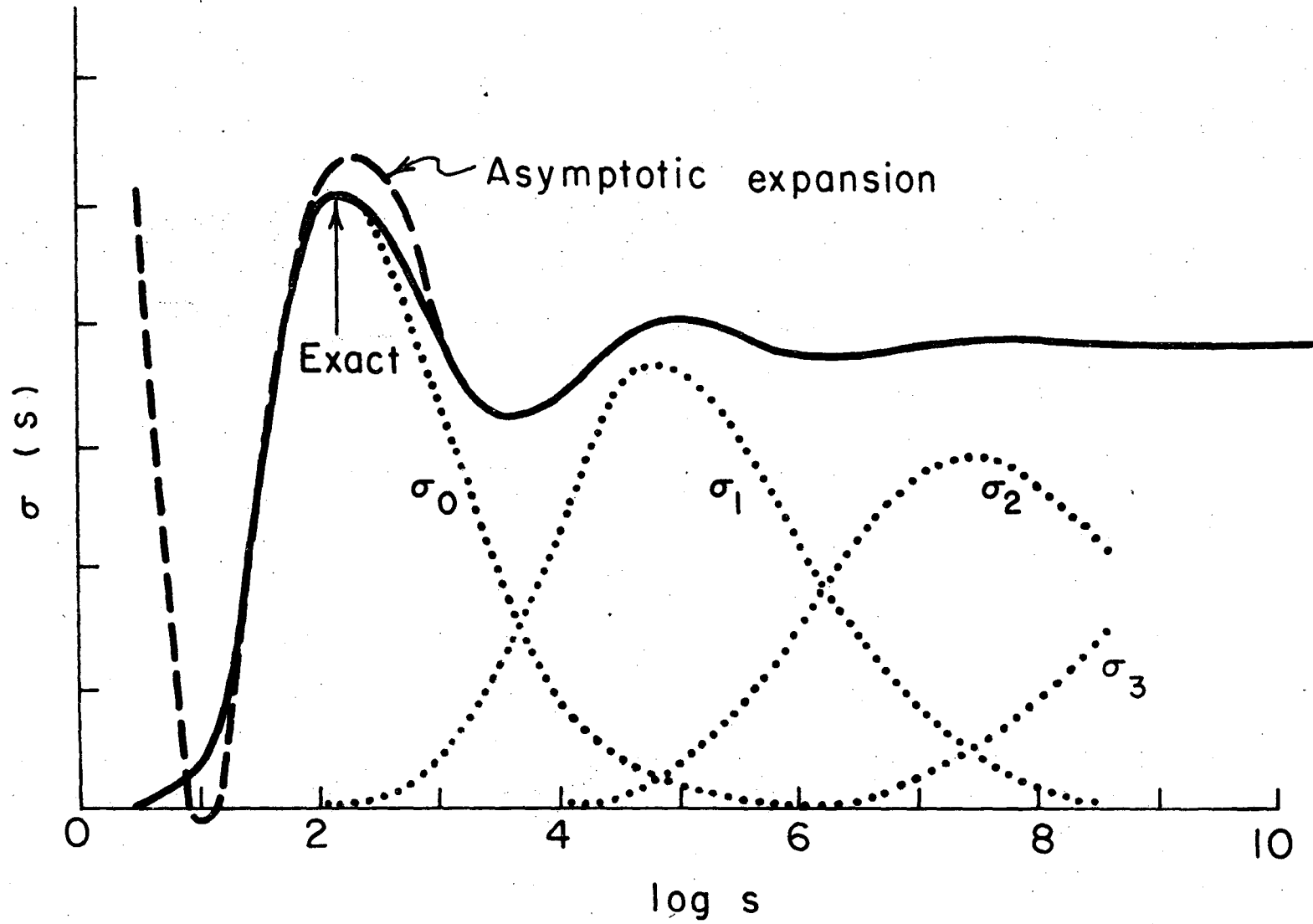
Fig. 5.

XBL745 - 3056
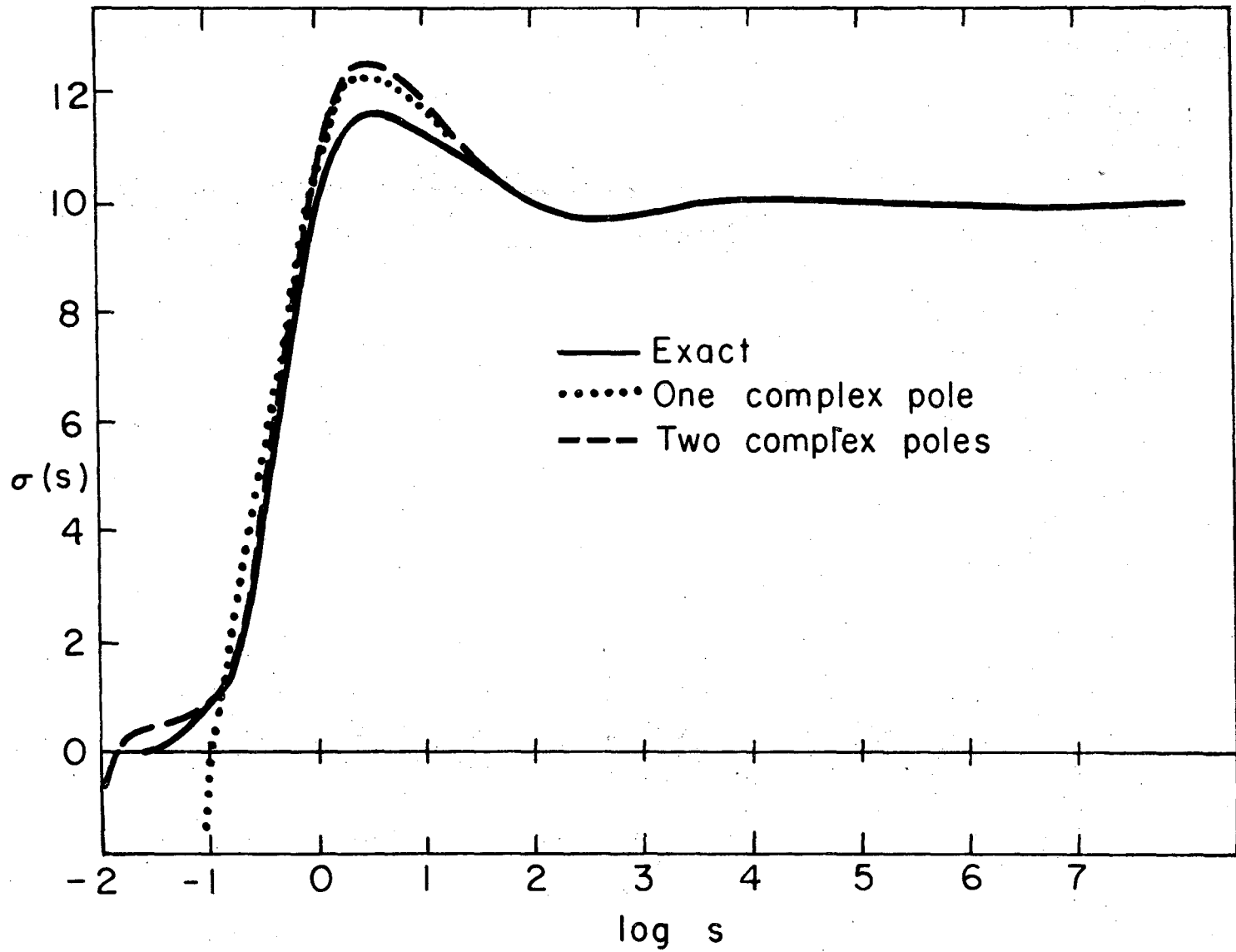
Fig. 6.
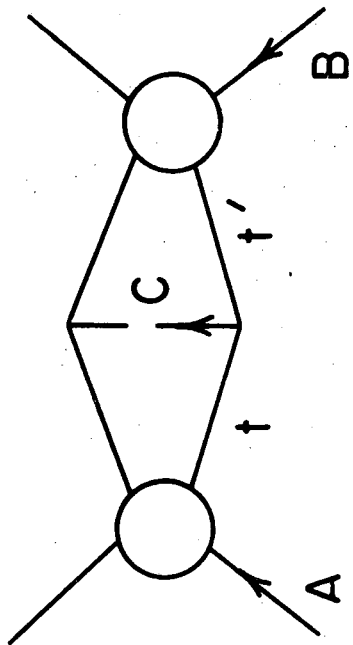
XBL745-3057

XBL745-3058

Fig. 7

Fig. 8.

XBL745-3059

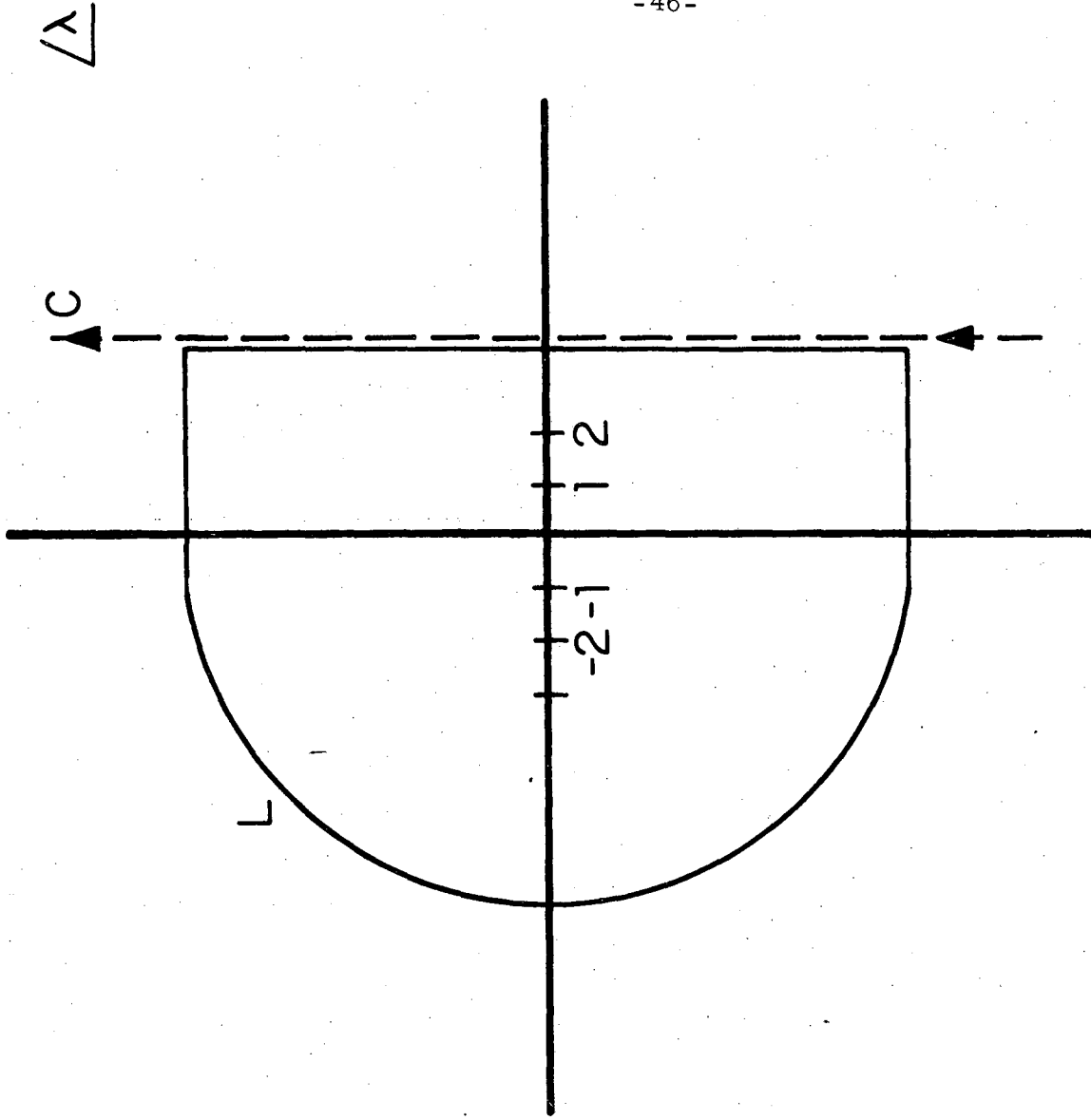Fig. 9.

-45-

XBL 746-3363

Fig. 10

XBL 746-3364

Fig. 11